OPTOELECTRONICS AND ADVANCED MATERIALS – RAPID COMMUNICATIONS Vol. 4, No. 12, December 2010, p. 1929 - 1932

Fabrication and dispersion measurement of photonic crystal fiber with central holes

JINHUI YUAN*, XINZHU SANG, CHONGXIU YU, JINLONG ZHANG, YUN TENG, XIANGJUNXIN, JINGWEI XING, GUIYAO ZHOU[a], SHUGUANG LI[a], LANTIAN HOU[a]

Key Laboratory of Information Photonics and Optical Communications (Beijing University of Posts and Telecommunications), Ministry of Education, P. O. Box163 (BUPT), 100876 Beijing, China

[a]Institute of Infrared Optical Fibers and Sensors, College of Information Science and Engineering, Yanshan University, Qinhuangdao 066004, China

Photonic crystal fiber (PCF) with central holes is designed and fabricated by extracting air from the central hole, and the integrated structure can be obtained by achieving the temperature field matching between the preform and furnace. The dispersion of fundamental mode is measured using the Michelson interference method, the phase differences between wave-apexes and vales in the interference spectrum are used to calculate the dispersion value, and the calculation error of dispersion due to the phase information conversion in Fourier-transform is decreased. The experimental result agrees well with that obtained by the Multi-pole method (MPM).

(Received November 4, 2010; accepted November 29, 2010)

Keywords: Photonic crystal fiber (PCF), Dispersion of fundamental mode, Michelson interference method, Multi-pole method (MPM)

1. Introduction

Because of optical transparency over a wide range of wavelengths and low loss, the photonic crystal fibers (PCFs) [1,2] with unique optical properties such as controllable dispersion and high nonlinearity mainly use the low-loss pure silica as the host material. The mechanisms of guiding light are mainly based on the total inner reflection (TIR) and photonic band gap (PBG). Since the PCFs were introduced to the technological community with the hope of revolutionizing the fiber optics industry, the development and application of PCFs open a broad range of devices such as devices for optical data processing in telecommunications systems and supercontinuum sources, and so on. However, the PCFs require a more complex fabrication process in comparison to conventional optical fibers [3], and there is a need for examining the processing dynamics of the fiber structure during the draw process in order to optimize the fabrication process. Different PCFs for specific applications can be fabricated by several methods such as extrusion, sol–gel formation [4], mechanical boring or milling [5, 6], and the "stack-and-draw" technique [7-11].

Recently, generation of ultrashort pulse and supercontinuum in comparatively short PCFs have been demonstrated, and the dispersion of PCFs has a great influence on the pulse and spectra characteristics. Therefore, accurate dispersion management has been required in high capacity ultrafast fiber optics. Up to now, the dispersion of PCFs has been measured using several methods such as the interferometric method, and the phase-shift method, and so on [12]. However, there exist some limitations in these methods. For example, an upper wavelength limit exists in the interferometric measurement, and the special detector is required. The phase shift method requires the use of multiple lasers or a wavelength-tunable laser, and a reference light is needed to eliminate the effect of the fiber length variation caused by temperature fluctuation if a longer fiber is used.

Here, the fabrication process of PCF with central holes including the material selection and the control of drawing velocity and temperature is shown. The final structure is influenced by fluctuations of air pressure, temperature and tension. The dispersion of fundamental mode is measured using the Michelson interference method. The interference spectrum is observed, and the phase differences between wave-apexes and vales in the interference spectrum are used to calculate the dispersion value, and the results show better consistence with that simulated by the Multi-pole method (MPM).

2. Fabrication of PCF

The preform stacked by capillaries with the same diameters of 0.4 mm is shown in Fig. 1 (a) and (b). These capillaries made of a kind of new-pattern glass tubes take on characteristics of higher temperature stabilization, stronger anti-pressure, lower material loss and well optical transmission. The capillaries are staked into the hexagon and arranged in triangular cells, and some additional capillaries with diameters of 0.2~0.25 mm are filled into the inter-space between cladding region with six rings and

coat-tube with diameter of 6.8 mm to keep compaction and stability of preform. The coat-tube and capillaries shows similar characteristics of temperature, especially, the melting points are at 1800 and 1780 ^{o}C, which ensure the inner and outer structures to be kept integration.

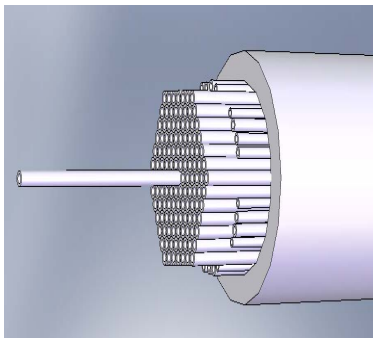

(a)

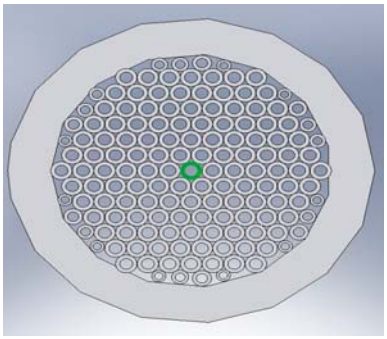

(b)

Fig. 1. (a) The three dimension preform stacked using capillary with the same sizes. (b) The two dimension plane structure of preform.

The optimal drawing velocity and temperature depend on the temperature field matching between the preform and furnace. The matching condition is achieved while the temperature of furnace can fall toward the softening temperature of silica glass to prevent the structure of preform from being distorted. By theoretical and experimental analysis, the corresponding drawing velocity and temperature are chosen to be 6.5 mm/min and 2145 K. Moreover, the preform is reduced by 200 times, and the central hole achieves up to 2 μm. The air pressures of central hole and cladding holes are adjusted through extracting air from central hole or infusing air into cladding holes, and the air pressure in central hole is kept lower than that in cladding holes within one standard atmosphere pressure in the process of fabrication. As presented in Fig. 1 (a), the central capillary is 8 cm longer than the surrounding ones to extract or infuse air conveniently to prevent the air from leaking into cladding holes or central hole. Fig. 2 shows the relations between diameter of central hole and air pressure in cladding holes and central hole. The diameter of central hole will diminish as increase of air pressure in cladding holes or decrease of air pressure in central hole, and the changing slopes are 0.2 μm per 0.1×10^5 Pa in the air pressure range of 1×10^5 to 2×10^5 Pa in cladding holes and 1×10^5 to 0 Pa in central hole.

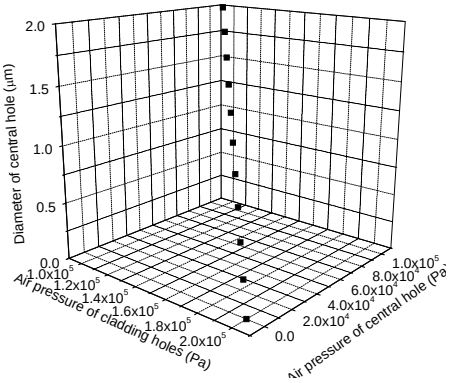

Fig. 2. The experimental data fit for diameter of central hole as functions of air pressure in cladding holes and central hole through extracting or infusing air in the range of one standard atmosphere pressure.

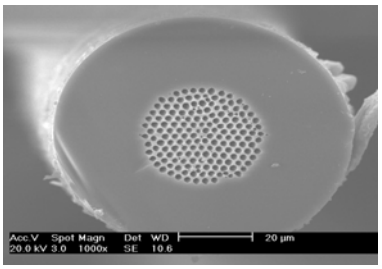

(a)

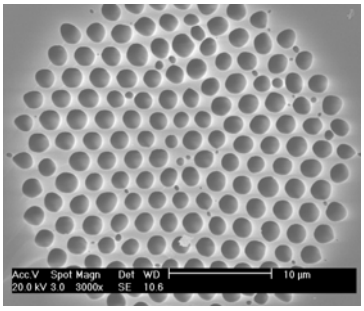

(b)

Fig. 3. (a) The whole SEM of cross-section structure of PCF. (b) The amplified cross-section of cladding and core region.

The scanning electron microscopy (SEM) of cross-section structure of PCF, which is fabricated through using improved stack and draw technology [16] and extracting air from central hole, is shown in Fig. 3. Fig. 3 (a) and (b) correspond to the whole outer and amplified inner cross-sections. Because there are existing some complicated factors on the arts and crafts including fluctuations of air pressure, temperature and tension, two air holes in the core region are formed during the fiber

drawing. Moreover, the cladding holes have some degree of deformation, and one of the air-holes in the first ring is much smaller than the others, which introduces birefringence to a certain extent.

3. Dispersion measurement of fundamental mode

The group-velocity dispersion *D* of fundamental mode is measured using Michelson interference method, as shown in Fig. 4 (a). The light source is a SC source with 3 dB bandwidth of 160 nm in the wavelength range from 820 to 980 nm generated by a highly nonlinear fiber. The incident light beam is kept at linear polarization state through a half-wave plate and polarization beam-split prism. The fundamental mode can be selectively excited through changing the distance between the input tip of the fiber and the lens to exactly adjust the angle between the input beam and the fiber axis. Two light beams pass through the reference-arm with a removable reflector and signal-arm with PCF tested and a fixed reflector, the corresponding light beams reflected encounter and intervene with each other at the 3 dB combined-beam plate, and the interference stripes in frequency domain can be observed by an optical spectrum analyzer (OSA), as shown in Fig. 4 (b). The attenuator 1 and 2 are used to adjust the intensities of light in two arms to enhance the modulation depth of stripes, and reduce the input power to depress the nonlinear effects in signal-arm.

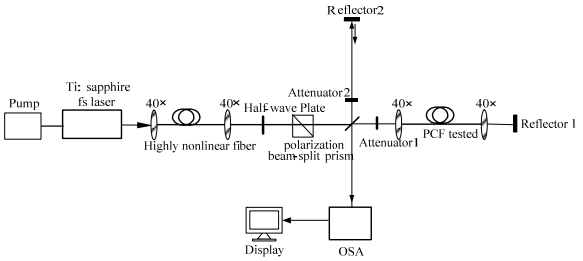

(a)

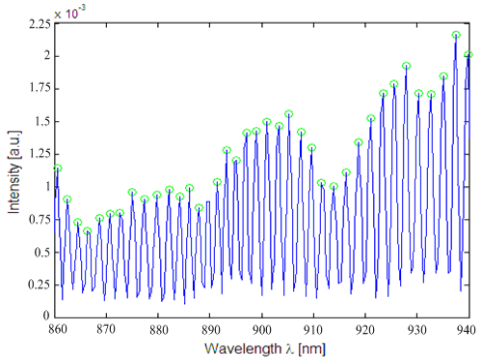

(b)

Fig. 4. (a) The experimental principle of measuring group-velocity dispersion of fundamental mode using Michelson interference method. (b) The interference spectrum observed by OSA.

In order to decrease the calculation error of dispersion due to phase information conversion in previous reported method based on Fourier-transform, the phase differences between wave-apexes and vales in the interference spectrum are used to calculate the dispersion value. The signal intensity of interference spectrum is normalized

$$I_{norm} = \frac{I_{out} - I_{air} - I_{fib}}{2\sqrt{I_{air} I_{fib}}} \tag{1}$$

The influence of noise outside the wave-band is eliminated through Fourier-transform

$$I_{norm}(\lambda) = I_{air}(\lambda) + I_{fib}(\lambda) + 2\sqrt{I_{air}(\lambda) I_{fib}(\lambda)}\cos\left(\beta_{fib} L_{fib} - \beta_{air} L_{air}\right) \tag{2}$$

where $\phi(\omega) = \beta_{fib}(\omega)\cdot L_{fib} - \beta_{air}\cdot L_{air}$, $\beta_{fib}(\omega)$ and β_{air} represent the propagation constants of light beam in fiber and air, and L_{fib} and L_{air} correspond to the propagation distance of light beam in fiber and air, respectively. $\phi(\omega)$ is expanded at the central wavelength λ_0 based on Taylor-formula.

$$\phi(\omega) = \phi_0 + \left[\beta_1 L_{fib} - \frac{d}{c}\right](\lambda - \lambda_0) + \frac{1}{2}\beta_2 L_{fib}(\lambda - \lambda_0)^2 + \frac{1}{6}\beta_3 L_{fib}(\lambda - \lambda_0)^3 + \cdots \tag{3}$$

$$\Delta\phi = k(\Omega_1 - \Omega_2) + \frac{1}{2}\beta_2 L_{fib}(\Omega_1^2 - \Omega_2^2) + \frac{1}{6}\beta_3 L_{fib}(\Omega_1^3 - \Omega_2^3) + \cdots \tag{4}$$

Here $k = \beta_1 L_{fib} - \frac{d}{c}$, $\Omega_1 = \lambda_1 - \lambda_0$, $\Omega_2 = \lambda_2 - \lambda_0$, d and c correspond to the length of reference-arm and light velocity in vacuum, respectively.

Through adjusting the fiber length, k =0 can be achieved. Moreover, the phase differences between successive maximums and minimums are $\pm 2\pi$. The condition $\lambda_1 > \lambda_2 > \lambda_0$ is satisfied in the normal dispersion region, and $\phi(\lambda_1) - \phi(\lambda_2) = -\pi$; similarly in the anomalous dispersion region, $\lambda_1 < \lambda_2 < \lambda_0$, and $\phi(\lambda_1) - \phi(\lambda_2) = \pi$. Based on above analysis, the matrix equation of $\Delta\phi$ can be obtained. Moreover, $\beta_2(\lambda)$ can be described as

$$\beta_2(\lambda) = \beta_2(\lambda_0) + \beta_3(\lambda_0)(\lambda - \lambda_0) + \frac{\beta_4(\lambda_0)}{2}(\lambda - \lambda_0)^2 + \frac{\beta_5(\lambda_0)}{6}(\lambda - \lambda_0)^3 \tag{5}$$

Neglecting the higher-order dispersion, the group-velocity dispersion D can be obtained from $D = -\frac{2\pi c}{\lambda^2}\beta_2$, and the corresponding dispersion

curve fitted linearly is shown in Fig. 5 (a) and (b).

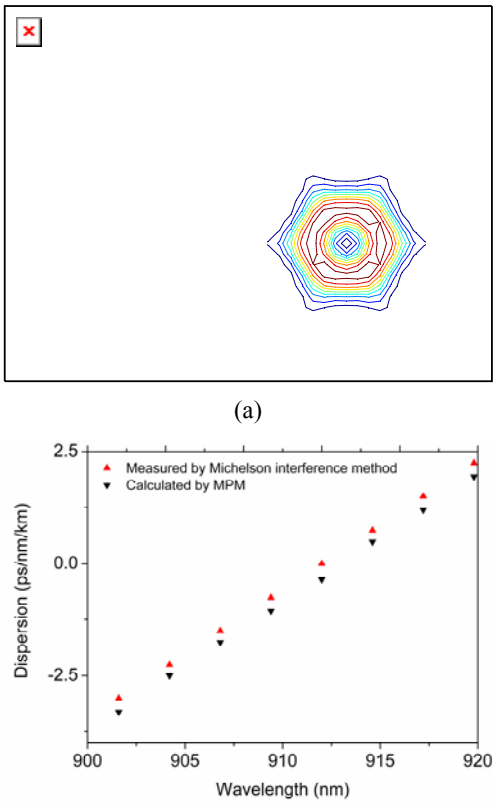

Fig. 5. (a) The group-velocity dispersion of fundamental mode as a function of wavelength, and (b) the amplified dispersion relation, insert showing the transverse field distribution of fundamental mode. The red up-triangle and black down-triangle line represents the dispersion curve measured by Michelson interference method and calculated by MPM, respectively.

As shown in Fig. 5 (a), the dispersion curves are nearly linear, and the value changes from -15 to 9 ps/nm/km in the wavelength range of 860 to 940 nm with zero dispersion wavelength of 913 nm. The insert shows the distribution of transverse field intensity in the fundamental mode, where the fundamental mode is a doublet of degenerate mode with electric field intensity reaching its maximum at the edge of the central hole and monotonically decreasing with the distance from the central region. Fig. 5 (b) shows the amplified part of Fig. 5 (a) in the wavelength range of 900 to 920 nm, the dispersion values change from -3.1 to 2.5 ps/nm/km with maximal difference between two curves only 0.41 ps/nm/km, and the accurate measurement is achieved.

4. Conclusions

The PCF is designed and fabricated by using the improved "stack-and-draw" technique and extracting air from central hole. The dispersion of fundamental mode is measured using the Michelson interference method, and the calculation error of dispersion due to phase information conversion in Fourier-transform is decreased by using the phase differences between wave-apexes and vales in the interference spectrum to calculate the dispersion value. The further works mainly concentrate on two aspects. The first one is to improve the arts and crafts and optimize the fiber design to fabricate PCFs with better performances. The second one is to use the PCFs for some applications such as generation of supercontinuum sources and frequency conversion.

Acknowledgments

This work is partly supported by the National Key Basic Research Special Foundation (2010CB327605 and 2010CB328300), National High-Technology Research and Development Program of China (2009AA01Z220), the key grant of Chinese Ministry of Education (No.109015), the discipline Co-construction Project of Beijing Municipal Commission of Education (YB20081001301), the Open Fund of Key Laboratory of Information Photonics and Optical Communications (Beijing University of Posts and Telecommunications), Ministry of Education, and the Specialized Research Fund for the Doctoral Program of Beijing University of Posts and Telecommunications (CX201023).

References

[1] P. St. J. Russell, Science **299**, 358 (2003).
[2] J. C. Knight, Nature **424**, 847 (2003).
[3] K. E. Framton, D.W. Hewak, World Intellectual Property Organization (PCT), WO 03/078339 A1, Sep. 25 (2003).
[4] N. F. Borelli, J. F. Wright, Jr, R. R. Wusirika, U.S. Patent 6 496 632, Dec. 17 (2002).
[5] C. Jackobsen, G. Vienne, T. P. Hansen, World Intellectual Property Organization (PCT), WO 03/078338 A2, Sep. 25 (2003).
[6] T. Hasegawa, U.S. Patent 6 766 088, Jul. 20 (2004).
[7] A. F. Benabid, J. C. Knight, World Intellectual Property Organization (PCT), WO 2004/001461 A1, Dec. 31 (2003).
[8] J. Broeng, S. E. Barkou, A. O. Bjarklev, World Intellectual Property Organization (PCT), WO 99/64903, Dec. 16 (1999).
[9] W. Belardi, World Intellectual Property Organization (PCT), WO 02/16980 A1, Feb. 28 (2002).
[10] P. J. Russell, World Intellectual Property Organization (PCT), WO 00/60388, Oct. 12 (2000).
[11] D. J. DiGiovanni, U.S. Patent 5 802 236, Sep. 1 (1998).
[12] L. G. Cohen, J. Lightwave Technol. **3**, 958 (1985).

*Corresponding author: yuanjinhui81@163.com